Role of vessel-to-prosthesis size mismatch in venous valve performance

Wei-Hsin Tien, PhD,[a] Xuefeng Zhao, PhD,[b] Henry Y. Chen, PhD,[c] Zachary C. Berwick, PhD,[c] Joshua F. Krieger, BS,[d] Sean Chambers, PhD,[d] Dana Dabiri, PhD,[e] *and* Ghassan S. Kassab, PhD,[b] *Taipei, Taiwan; San Diego, Calif; Bloomington, Ind; and Seattle, Wash*

ABSTRACT

Background: Efforts to treat chronic venous insufficiency have focused on the development of prosthetic venous valves. The role of prosthetic valve-to-vessel size matching has not been determined. The purpose of this investigation was to assess the effect of size mismatching on venous valve function and to establish a mismatch limit that affects valve hemodynamic performance and venous wall stress to improve future valve designs and implants.

Methods: Flow dynamics of prosthetic venous valves were studied in vitro using a pulse duplicator flow loop. Valve performance based on flow rate and pressure measurements was determined at oversizing ratios ranging from 4.2% to 25%. Valve open area ratios at different size mismatching ratios were investigated by image analysis. Finally, a wall stress analysis was used to determine the magnitude of circumferential (hoop) stress in the venous wall at various degrees of oversizing.

Results: Our findings indicate that valve regurgitate volume, closing time, and pressure difference across the valve are significantly elevated at mismatch ratios greater than ~15%. This is supported by increases in regurgitate velocity and open area relative to valves tested at near-nominal diameters. At this degree of size mismatch, the wall stress is increased by a factor of two to three times relative to physiologic pressures.

Conclusions: These findings establish a relationship between valve size matching and valve hemodynamic performance, including vessel wall stress, which should be considered in future valve implants. The size of the prosthetic valve should be within 15% of maximum vein size to optimize venous valve hemodynamic performance and to minimize the hoop wall stress. (J Vasc Surg: Venous and Lym Dis 2017;5:105-13.)

Clinical Relevance: The effect of size mismatching on venous valve function and mismatch limit that affects valve hemodynamic performance and venous wall stress is investigated. Valve regurgitate volume, closing time, and pressure difference across the valve are significantly elevated at mismatch ratios >15%. The wall stress is increased by a factor of two to three times larger than that induced by physiologic pressures. To improve future valve implants for treatment of chronic venous insufficiency, vessel wall stress should be considered. A size mismatch <15% is needed to optimize venous valve hemodynamic performance and to minimize the hoop wall stress.

The development of prosthetic venous valves for the treatment of chronic venous insufficiency has been a topic of significant interest but has yet to yield a successful product. Several valve designs have been tested with unfavorable durations of competency.[1-4] The primary failure modes of venous valves are thrombosis and fibrosis surrounding the valve, which compromise patency or competency or both. Given the complex etiology of chronic venous insufficiency, a number of variables need to be optimized to develop a successful prosthetic venous valve.

The size mismatch between the vein and the prosthetic valve has received little attention in valve design, and its contribution to valve function is unknown. Size mismatch of the valve can alter the leaflet profile because of deformation of the frame as well as elevate vein wall stress. Compression of stented valves due to size mismatch increases the propensity for leaflet-wall contact as suggested by several studies that identified this as a failure mode.[5,6] Such alterations in valve spatial profiles may adversely affect valve mechanics and render even the best designs incompetent. Despite these potential implications, the degree to which size mismatch becomes a critical factor in valve performance has yet to be determined.

From the Department of Mechanical Engineering, National Taiwan University of Science and Technology, Taipei[a]; California Medical Innovations Institute,[b] and the Research and Development, 3DT Holdings, LLC,[c] San Diego; Research Engineering, Cook Medical, Bloomington[d]; and the Department of Aeronautics and Astronautics, University of Washington, Seattle.[e]

This work was funded by Cook Medical, Inc. Cook Medical, Inc had no involvement in the study design; collection, analysis, and interpretation of data; manuscript writing; or the decision to submit the manuscript for publication.

Author conflict of interest: none.

Additional material for this article may be found online at www.jvsvenous.org.

Correspondence: Ghassan S. Kassab, PhD, California Medical Innovations Institute, 11107 Roselle St, San Diego, CA 92121 (e-mail: gkassab@calmi2.org).

The editors and reviewers of this article have no relevant financial relationships to disclose per the Journal policy that requires reviewers to decline review of any manuscript for which they may have a conflict of interest.

2213-333X

http://dx.doi.org/10.1016/j.jvsv.2016.08.004

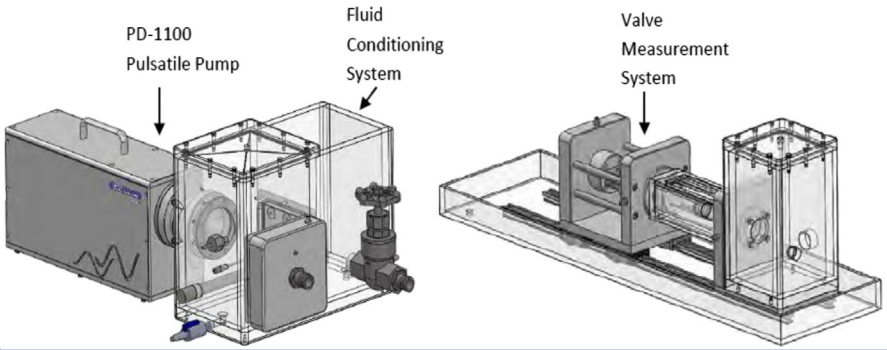

Fig 1. The pulse duplicator apparatus and system that consist of the pulsatile pump, flow conditioning system, and valve measurement system.

Previous investigations have shown that the solid stress acting on the vein wall plays an important role in inducing hyperplasia and remodeling[7-11] and may explain some of the adverse histologic findings surrounding valve leaflets.[3] Hence, oversizing of venous valves on frames with large radial force can probably promote stress-induced inflammation and tissue remodeling.[12] Although solutions in the past have focused on improving biocompatibility of leaflet materials or pretreatment to prevent inflammation,[13] no consideration has been given to the effect of size matching on vessel injury and how these factors may be optimized to attenuate inflammatory responses. Accordingly, we hypothesized that venous valve size mismatch plays a significant role in vascular injury responses and valve performance that can lead to valve failure. This study leverages both bench studies and computational methods to identify an appropriate range of valve size mismatch that preserves valve mechanics while minimizing hoop wall stress to aid in improvement of prosthetic venous valve performance.

METHODS

In vitro experiment setup. A pulse duplicator was used (BDC Laboratories, Wheat Ridge, Colo) to generate the pulsatile flow to mimic physiologic conditions. Physiologic pressures and flow conditions across the valve were duplicated and recorded for subsequent analysis. The system consisted of three components: (1) pulsatile diaphragm pump, (2) flow regulation system, and (3) test section (Fig 1). The computer-controlled and servo motor-driven pump (PD-1100; BDC Laboratories) provided control over the waveform and frequency of fluid flow. The flow system provided flow directional and mean pressure control. The pressure difference created by the pulsatile pump during valve closure was controlled by the pressure differential control valve. Mean pressure of the system was controlled by a needle valve distal to the valve testing chamber that allowed regulation of outflow resistance.

The test section consisted of a square container made of Plexiglas and a round glass tube to mimic the geometry of the vessel. The entire test section was then mounted in the system for the valve testing. Two pressure transducers were used to measure the upstream and downstream pressure of the test section to evaluate the valve performance. An ultrasound flow probe (ME13PXN; Transonic Systems, Ithaca, NY) was mounted upstream to provide flow rate measurement of the system. For experiments in this study, the mean flow rate was set at 0.35 L/min at 15 beats/min; the peak pressure difference was adjusted to 2 mm Hg, with inflow pressure being dependent on the pressure differential. The mean flow rate was selected on the basis of the calculation in the study by Fronek et al.[14] This flow rate was also used in the prosthetic venous valve study by Rittgers et al.[15] To mimic the viscosity of the blood, the working fluid was a solution of glycerol and water at a volume ratio of 2:3 to yield a viscosity of 3.7 cP at 25°C with a 1.4 refraction index. The blood-mimicking solutions have been used in our previous published works.[16,17] At the testing condition, the Reynolds and Womersley numbers were 360 and 4.5, respectively.

The bioprosthetic valve used for this study was provided by Cook Biotech Inc (West Lafayette, Ind). The valve was a third-generation bioprosthetic venous valve (BVV3) with a 12-mm nominal diameter and valve leaflets made from small intestinal submucosa.[3] The valve leaflets were half the length of the frame. A total of four valves were tested with each size glass tube. For the size mismatching tests, six undersized glass tubes were made with inner diameter of 9 mm, 9.5 mm, 10 mm, 10.5 mm, 11 mm, and 11.5 mm. Pressure and flow rate data of four cycles were recorded for each case at 5 KHz acquisition rate, and end-view videos were captured to visualize the movements of the valve. From the end-view snapshot with the valve fully opened, the open area ratio was calculated.

Statistical analysis. Data in Table I are presented as mean ± standard error. Statistical comparisons were

Table I. Valve performance of various geometric and hemodynamic parameters

Parameter	9.0 mm	9.5 mm	10.0 mm	10.5 mm	11.0 mm	11.5 mm
Closing volume, mL	0.37 ± 0.08[a]	0.38 ± 0.08[a]	0.30 ± 0.08	0.32 ± 0.06	0.19 ± 0.01	0.17 ± 0.01
Closing time, seconds	0.22 ± 0.03[a]	0.24 ± 0.03[a]	0.20 ± 0.03	0.2 ± 0.02	0.15 ± 0.01	0.15 ± 0.01
Closing volume time/cycle, %	5.5 ± 0.70[a]	6.0 ± 0.76[a]	5.0 ± 0.74	5.2 ± 0.55	3.8 ± 0.13	3.7 ± 0.11
Leakage volume, mL	0.80 ± 0.19[a]	0.67 ± 0.15[a]	0.46 ± 0.09	0.35 ± 0.06	0.32 ± 0.07	0.30 ± 0.08
Regurgitate fraction volume, %	5.2 ± 1.26[a]	4.8 ± 1.06[a]	3.3 ± 0.65	2.9 ± 0.50	2.2 ± 0.31	2.0 ± 0.36
Regurgitate velocity, cm/s	4.8 ± 1.27[a]	4.0 ± 0.93[a]	2.9 ± 0.59	2.1 ± 0.47	1.9 ± 0.28	1.7 ± 0.30
Stroke volume, mL	23 ± 0.5[a]	22 ± 0.3[a]	23 ± 0.2[a]	23 ± 0.3[a]	24 ± 0.2[a]	24 ± 0.5
Stroke volume time, %	57 ± 0.6	57 ± 0.6	58 ± 0.5	58 ± 0.9	58 ± 0.9	58 ± 1.5
Systolic duration, %	62 ± 0.8	63 ± 0.7	63 ± 0.5	63 ± 1.0	62 ± 0.9	62 ± 1.4
Mean forward flow, mL/s	10. ± 0.2	9.9 ± 0.2	9.9 ± 0.1	10 ± 0.3	10 ± 0.3	11 ± 0.4
Effective orifice area, mm^2	14 ± 0.5	18 ± 0.3	18 ± 0.3	18 ± 0.6	18 ± 1.2	19 ± 0.6
Open area ratio, %	44 ± 2.6[a]	39 ± 2.0[a]	38 ± 1.5[a]	30 ± 1.4	30 ± 1.4	28 ± 1.4
Cross-sectional area, mm^2	28 ± 1.7	28 ± 1.4	30 ± 1.2	26 ± 1.2	28 ± 1.3	29 ± 1.5

[a] $P < .05$.

made by one-way analysis of variance for between-group analyses. For all statistical comparisons, $P < .05$ was considered statistically significant.

Computational hoop stress analysis. Computational stress analysis was conducted to investigate the contribution of size mismatch to the hoop stress (ie, the stress along the circumferential direction of a vessel) experienced by the vessel wall relative to the physiologic stress associated with venous blood pressure. The computational analysis consisted of the following steps, which are summarized in a flow chart (Fig 2). First, the elastic property (ie, intrinsic material property relating deformation and induced stress, such as elastic stiffness) of a canine iliac vein was identified on the basis of the experimental data of normal vein diameters vs intramural pressure and axial force vs axial stretch in a combined inflation-extension experiment.[18] The details of the material constitutive law and mathematical derivation can be found in the Appendix (online only). Subsequently, the pressure-diameter curve (an indirect measurement of the elastic property of cylindrical structures, such as blood vessels) of veins of various sizes was predicted by assuming that the elastic property is independent of vein size. In this process, we also assumed that there is constant ratio between the initial wall thickness of veins and the initial diameter (i.e., wall thickness/inner diameter = 1/20).[19] The stress-free inner diameter of the veins ranged from 6.0 to 12.0 mm at an interval of 0.2 mm.

For individual veins of various diameters, we then determined the index of size mismatch as $\frac{d_{frame}-d_{vein}^{max}}{d_{frame}} \times 100\%$, ie, the percentage difference between the nominal diameter of the valve frame ($d_{frame} = 12$ mm) and the maximum inner diameter of the vein under 100 mm Hg blood pressure d_{vein}^{max}(axial stretch $\lambda_z = 1.5$). Next, the final inner diameter of the vein after the valve is deployed, which is identical to the final valve frame diameter, was determined by identifying the static equilibrium state (ie, a balance between internal and external forces) between the vein and the frame. At this equilibrium state, the internal force in the vessel wall must be in balance with the external load exerted on the internal surface of the vein, which accounts for both the resultant radial force of the frame and the physiologic blood pressure. Specifically, this was determined by finding the intersection point between the pressure-diameter curve of the valve frame and that of the vein, at which both vein and frame have identical diameter and pressure. Consequently, physiologic and stented hoop stresses, σ_θ^{physio} and σ_θ^{stent}, respectively, were determined for the three physiologic blood pressures (ie, 20, 30, and 40 mm Hg) from which the hoop stress ratio was calculated as $\sigma_\theta^{stent}/\sigma_\theta^{physio}$. In a ~180-cm standing human, the pressure gradient is 0.77 mm Hg per centimeter from the right atrium. This suggests that at the common femoral, we expect mean pressures around 40 mm Hg. According to Meissner et al,[20] the lower extremity pressure can change from 100 mm Hg to a mean pressure of 22 mm Hg within 7 to 12 steps when walking. These pressures were therefore selected on the basis of these assumptions regarding the vein dimensions at the cited pressure range.

It is noted that the raw data of valve frame stiffness were radial force vs diameter. To superimpose the effects of venous blood pressure and the contact force by the valve frame, we first translated radial force to equivalent pressure by assuming the contact force is uniformly distributed on the effective area distended by the frame, according to the formula $P_{frame} = F_{radial}/(\pi DL)$, where D, L, and F_{radial} are the diameter, length, and radial force of the valve frame.

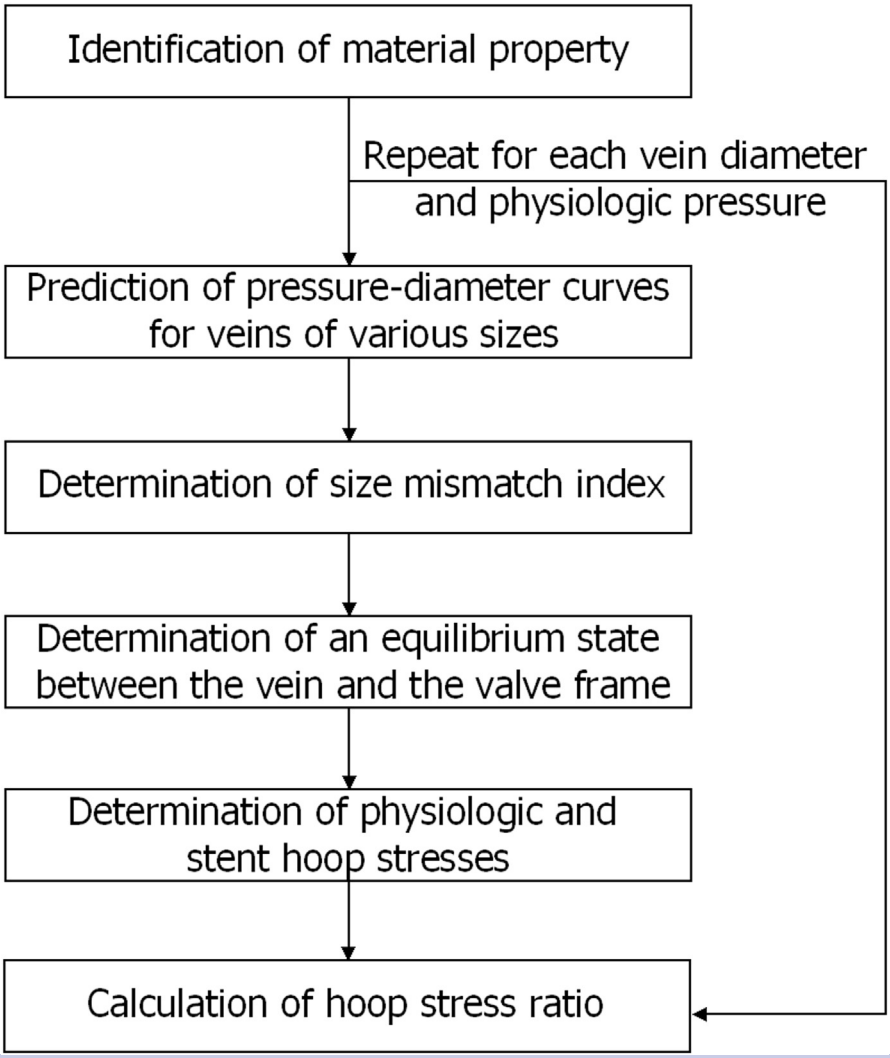

Fig 2. Flow chart of computational stress analysis to determine the effect of size mismatch on hoop stress ratio (stress due to valve frame relative to physiologic pressure-induced stress).

RESULTS

In vitro experiments. In the 9.5-mm glass tube, the valve open area ratio was significantly larger compared with the 11-mm inner diameter case (Table I; $P < .05$). In addition, the leaflets touched the vessel wall during the opening phase and formed an abrupt angle during the closing phase, in contrast to the smooth curved profile in the other two cases. Fig 3 shows the end view for all the cases. The valve open area ratios were roughly the same for the cases of 11.5 mm (4.2% mismatch), 11 mm (8.3%), and 10.5 mm (12.5%). The open area ratios were significantly larger for the cases of 10 mm (16.7%), 9.5 mm (20.8%), and 9 mm (25%), and the leaflet profiles during opening were different from the previous cases (Table I; $P < .05$).

Table I summarizes the valve performance comparison calculated from the pulse duplicator data. With size mismatching >20%, the valve had higher reflux volume (>100% increases between 25% and 4.2% case) but also had a larger open area ratio (>40% increase between 25% and 4.2% case). The total regurgitate volume (Fig 4) showed a linear increase of the reflux volume when size mismatching is <15%, with a step increase when the size mismatching is >15%. The closing time results (Table I) showed that the valve closes more slowly at size mismatch >15%. The opening area of the valve (Fig 3; Table I) increased significantly with size mismatching >15%. These results correlate with the visual observation in Fig 3, which showed that the leaflets of the valve deformed abnormally when the size mismatching was >15%.

Fig 4 demonstrates two key trends in valve performance with increases in size mismatching. Specifically, inward puckering of the valve significantly increases peak pressure differential, which represents the amount of resistance to forward flow that relates to the efficiency

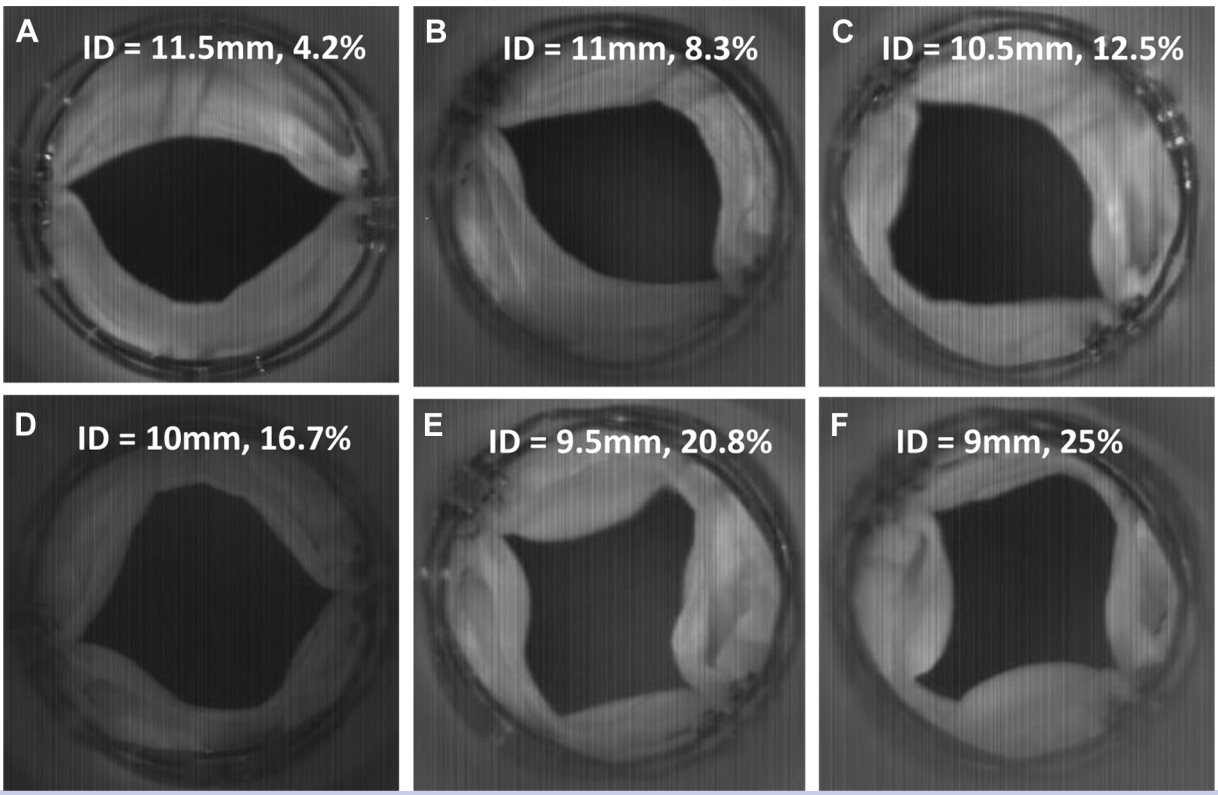

Fig 3. Snapshots of end view of the size mismatching valve tests during full valve opening. **A,** Inner diameter (*ID*) = 11.5 mm, 4.2% size mismatching. **B,** ID = 11 mm, 8.3% size mismatching. **C,** ID = 10.5 mm, 12.5% size mismatching. **D,** ID = 10 mm, 16.7% mismatching. **E,** ID = 9.5 mm, 20.8% size mismatching. **F,** ID = 9 mm, 25% size mismatching.

of the prosthetic valve. When the mean forward flow is approximately the same, the effective orifice area therefore decreases as the size mismatching ratio increases. This indicates that the valve becomes less efficient and causes more energy loss. Not only does increasing size mismatching impair opening, it also attenuates the ability of the valve to close as noted by the upward inflection of the relationship between total regurgitate volume and size mismatching (Fig 4, *B*).

Hoop stress. The estimated elastic parameters were $C = 0.0026$ kPa, $a_1 = 3.407$, $a_2 = 1.343$, and $a_4 = 1.152$. Fig 5 demonstrates the determination of the equilibrium state between the valve frame and the vein by intersecting the pressure-diameter curves of the frame and individual vein for blood pressures of 20, 30, and 40 mm Hg. Given that the pressure-diameter curve of the valve frame does not take into account physiologic blood pressure, it was translated toward the right by the

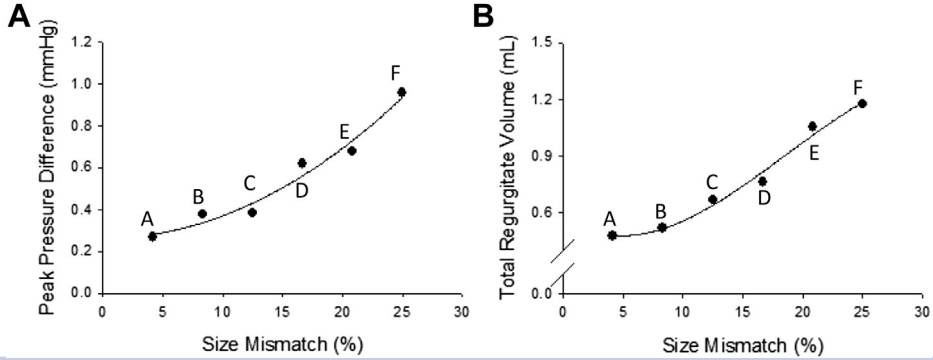

Fig 4. Peak pressure difference **(A)** and total regurgitate volume **(B)** as a function of vein/stent size mismatch. For *A* to *F* in the figure: *A*, inner diameter (ID) = 11.5 mm, 4.2% size mismatching; *B*, ID = 11 mm, 8.3% size mismatching; *C*, ID = 10.5 mm, 12.5% size mismatching; *D*, ID = 10 mm, 16.7% size mismatching; *E*, ID = 9.5 mm, 20.8% size mismatching; *F*, ID = 9 mm, 25% size mismatching.

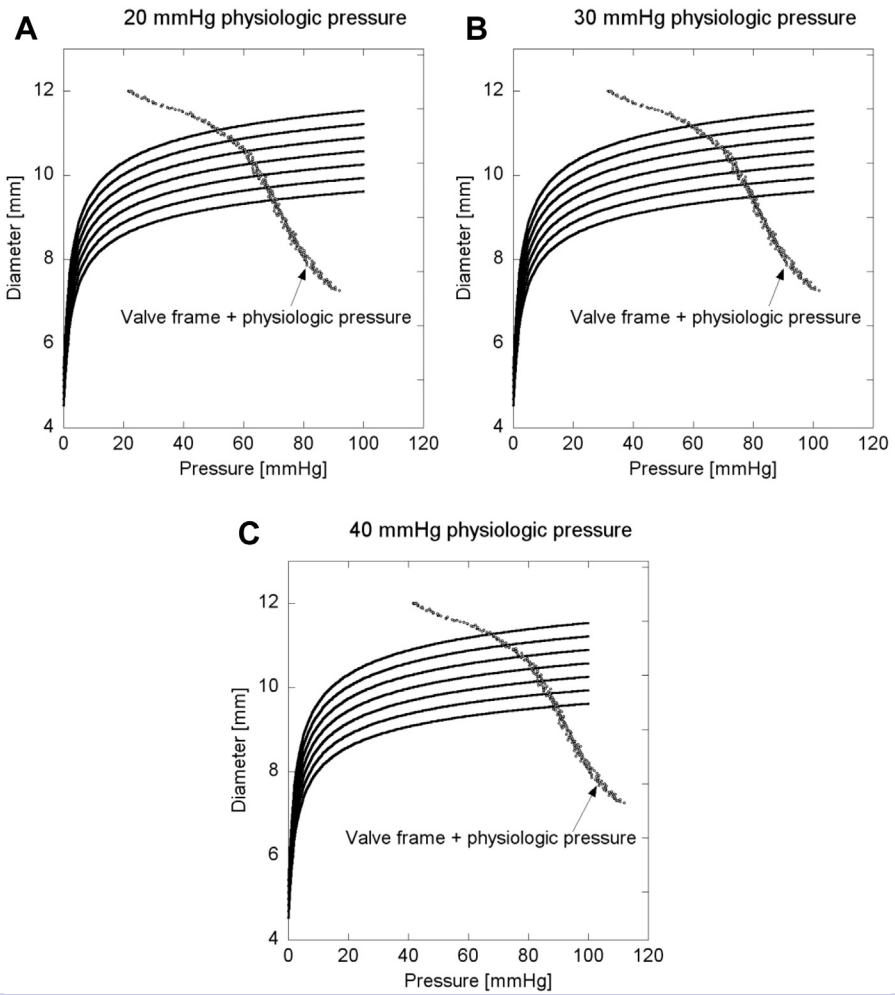

Fig 5. Determination of the equilibrium state between valve frame and veins of various inner diameters with the consideration of various physiologic blood pressures: **(A)** 20 mm Hg; **(B)** 30 mm Hg; **(C)** 40 mm Hg. The original pressure-diameter curve of the valve frame is translated to the right by the amount of corresponding physiologic pressure.

amount corresponding to physiologic blood pressure to account for the deformation of veins due to intraluminal pressure.

Table II lists the maximum inner diameter d_{vein}^{max} of the veins that have a positive size mismatch (ie, valve oversizing) and corresponding size mismatch and hoop stress ratio for the considered physiologic blood pressures. The d_{vein}^{max} ranges from 9.6 mm to 11.8 mm, and the size mismatch ranges from 1.24% to 19.9%. Fig 6 demonstrates the effect of size mismatch on the hoop stress ratio for the three different blood pressures. For each venous blood pressure, the stress ratio increases monotonically as the size mismatch increases. Moreover, the stress ratio decreases as physiologic blood pressure increases. For physiologic blood pressure of 20 mm Hg, the stress ratio reached 3.0 at a size mismatch of 6.6%. For the physiologic blood pressure of 30 mm Hg, a stress ratio of 3.0 was reached at the largest size mismatch of 20%. For 40 mm Hg blood pressure, the maximum stress ratio was 2.5.

DISCUSSION

The major conclusion is that when size mismatching is >15%, the valve performance tends to deteriorate significantly. The higher reflux volume indicates poor valve sealing during the closed phase. In a size-matched valve, the valve frame is fully expanded. At the valve closed phase, the coaptation from the free edges of the top and bottom leaflets has no leak points. In a size-mismatched valve, the leak points are formed because of the puckering of the valve leaflets. The puckering for the size-mismatched valves indicates additional deformation on the leaflets, which also causes slower closing time. This finding is in agreement with the results reported by Pavcnik et al,[5] in which nine percutaneous autogenous venous valves were transplanted in an ovine model, and the size mismatching ranged from −3% to 19%. Of the nine valves implanted, only one had a size mismatch >15%, and it was the only valve with regurgitate flow at implantation and 3-month follow-up.

Table II. Maximum inner diameter d_{vein}^{max} of the veins that have a positive size mismatch (ie, valve oversizing)

d_{vein}^{max}, mm	9.61	9.93	10.2	10.6	10.9	11.2	11.5	11.8
Size mismatch, %	19.9	17.3	14.6	11.9	9.25	6.58	3.91	1.24
Hoop stress ratio, –								
20 mm Hg	3.90	3.75	3.53	3.44	3.32	2.99	2.72	2.31
30 mm Hg	3.0	2.9	2.85	2.74	2.57	2.41	2.20	1.92
40 mm Hg	2.46	2.37	2.33	2.28	2.11	1.96	1.84	1.57

The valve efficiency deteriorates with increasing size mismatch. Inefficient valve function leads to reflux and flow stasis. The failure mode of valve may relate to inflammatory response, which may result in thrombosis to block flow and impede leaflet motion. Inefficient valve function is observed from the comparison of the effective orifice area to the actual valve cross-sectional area in Table I. Although the valve open area ratio during valve opening phase was larger for larger size mismatch (at approximately the same cross-sectional area), the effective orifice area decreased when the size mismatch increased. The large open area ratio is also not preferable for prosthetic valves because it raises concerns that the leaflets could contact the host vessel wall[1] and cause local thrombosis due to leaflets being forced against the walls of the conduit with every valve cycle.[21] For a prosthetic valve, the allowable open area should be smaller than that of native valves.[22] Native valves have a sinus pocket that can expand significantly,[23] which was not incorporated in the present prosthetic valves. The valve implanted location should be the vein section with normal size and no sinus pocket, and the open area should be smaller to compensate for this difference. These assertions require further validation in vivo before clinical translation.

Remodeling of venous wall may occur when the vessel is exposed to elevated venous blood pressure.[8-11] Choy et al[8] observed nonuniform axial and circumferential remodeling of large coronary veins in response to ligation and documented a 2.5-fold increase of mean venous pressure (20 to 50 mm Hg). Hayashi et al[24] investigated biomechanical response of femoral vein to chronic elevation of blood pressure in rabbits. They observed a twofold increase of blood pressure within 2 weeks after operation. For chronic remodeling, stress ratio >3 is likely to induce injury response and hyperplasia. This is based on studies by our group[7] demonstrating that pressures of 60 mm Hg promote intimal hyperplasia in veins that normally experience <20 mm Hg. The physiologic stress level was based on the supine venous pressure of 20 mm Hg.[23,25,26] During the standing position, the venous pressure can be significantly higher[27] and hence the reason to consider higher pressures (30 and 40 mm Hg) in the simulations. Because a typical person is in supine (sleeping) position 6 to 8 hours continuously per day, while standing only 0.1 to 1 hour at a time, the supine position is likely to be more relevant with respect to tissue remodeling.

Our findings indicate that valve performance is diminished by increases in regurgitate volume, closing time, and peak positive pressure difference at size mismatch >15%. In addition, the risk of stress-induced vessel inflammatory response and remodeling has to be taken into account for size mismatch >20%. Collectively, a size mismatch below 15% is advisable to minimize perturbations of normal fluid and solid stresses.

Limitations. A major limitation of the current experimental study is that the vessel is simulated by a solid glass tube, which is different from the normal compliant vein vessel wall. The compliance of the vessel wall may accommodate the valve frame, and size change may not be as severe as shown in the in vitro experiments. On the other hand, the abrupt change in the vessel diameter because of the valve frame could cause significant flow deceleration and flow stagnation regions. The stress between the vessel wall and the frame will

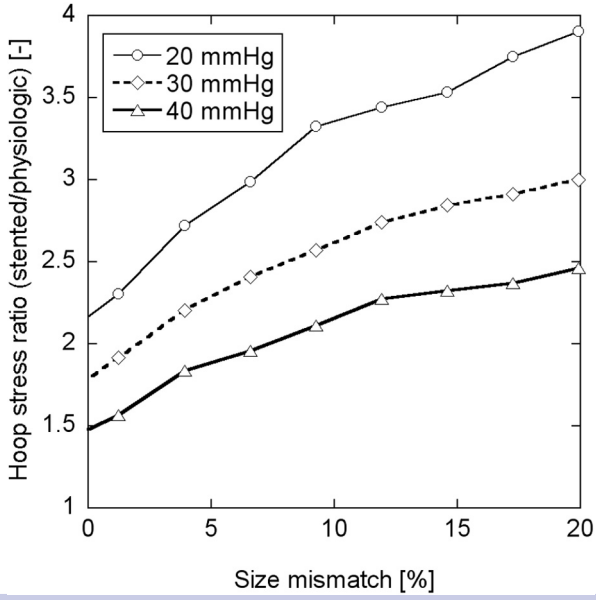

Fig 6. Effect of size mismatch on the hoop stress ratio (stent stress/physiologic stress).

determine the actual size mismatch. A more realistic test can be performed using a transparent compliant material that mimics the vein vessel. The material properties of the blood vessel (especially as thin as the vein), however, are not easy to replicate. Therefore, only stiff transparent tubes were used to simplify data interpretation and to avoid confounding artifacts. We have shown that there is some tolerance to mis-sizing (within 15%) beyond which the mechanical performance of the valve may degrade. From an engineering point of view, the goal is to expand the range of this tolerance in future iterations of the valve design. Although validation of these results awaits future large animal studies, the intuitive results appear reasonable. Our results are likely to provide a conservative estimation of the size mismatch limit for the valve implantation. Future validation of these bench findings requires in vivo studies in large animal models in conjunction with intravascular imaging to visualize the dynamics of the valve and the vein wall.

There were several assumptions made in the computational analysis, given that experimental data are lacking for such a broad range of vein diameters of interest in this study. First, the elastic property was assumed to be identical for veins of different sizes. Second, we assumed a scaling relation between the wall thickness and diameter of veins (ie, wall thickness/diameter = 1/20), which is documented for large veins (diameter >9 mm) of humans.[20] Third, we did not consider residual strain for veins; that is, the stress-free configuration is identical to the load-free configuration. This assumption is reasonable for veins that are thin walled and relatively compliant. As a more complete database of the morphologic and material properties is established for veins, a more comprehensive study may be undertaken to further understand the influence of valve size mismatch on vein wall stress. Moreover, experimental and computational analyses that are vein specific are important because the intrinsic material properties of veins may be different for various veins and species. Although future refinements can be made, this computational stress analysis lays a foundation for a thorough understanding of the importance of size mismatch for prosthetic venous valves.

CONCLUSIONS

This is the first study of the influence of size mismatch of prosthetic valve to vein. The effects on both the fluid mechanics and solid mechanics of prosthetic valve inside a vessel were investigated using in vitro tests and stress analysis on measured force data. The results show that size mismatch <15% does not significantly affect the function of a venous valve. Above 15% size mismatch, the flow around the valve and the valve motion are altered significantly, causing increase in reflux volume, closing time, and peak positive pressure difference. The hoop stress analysis shows that a size mismatch <15% is desirable to maintain a stress ratio <3. Based on the in vitro test results combined with the hoop stress analysis results, the recommended size mismatching of the prosthetic valve and the target vessel should be <15% to ensure normal performance of the valve and to minimize adverse vessel wall remodeling.

This research was supported by 3DT Holdings, LLC and Cook Medical. We wish to acknowledge the excellent technical expertise of Dr Chad Johnson and Mrs Martha Spicer in producing the valve prototypes. We also thank Dr S. Raju for his valuable clinical feedback.

AUTHOR CONTRIBUTIONS

Conception and design: W-HT, HC, ZB, DD, GK
Analysis and interpretation: XZ, HC, ZB
Data collection: W-HT, ZB
Writing the article: W-HT, XZ, HC
Critical revision of the article: ZB, JK, SC, DD, GK
Final approval of the article: W-HT, XZ, HC, ZB, JK, SC, DD, GK
Statistical analysis: XZ, ZB
Obtained funding: GK
Overall responsibility: GK

REFERENCES

1. de Borst GJ, Moll FL. Percutaneous venous valve designs for treatment of deep venous insufficiency. J Endovasc Ther 2012;19:291-302.
2. Zervides C, Giannoukas AD. Historical overview of venous valve prostheses for the treatment of deep venous valve insufficiency. J Endovasc Ther 2012;19:281-90.
3. Pavcnik D, Uchida B, Kaufman J, Hinds M, Keller FS, Rösch J. Percutaneous management of chronic deep venous reflux: review of experimental work and early clinical experience with bioprosthetic valve. Vasc Med 2008;13:75-84.
4. Bergan JJ. The vein book. Oxford: Oxford University Press; 2007.
5. Pavcnik D, Yin Q, Uchida B, Park WK, Hoppe H, Kim MD, et al. Percutaneous autologous venous valve transplantation: short-term feasibility study in an ovine model. J Vasc Surg 2007;46:338-45.
6. Pavcnik D, Uchida BT, Timmermans HA, Corless CL, O'Hara M, Toyota N, et al. Percutaneous bioprosthetic venous valve: a long-term study in sheep. J Vasc Surg 2002;35:598-602.
7. Choy JS, Kassab GS. A novel strategy for increasing wall thickness of coronary venules prior to retroperfusion. Am J Physiol Heart Circ Physiol 2006;291:H972-8.
8. Choy JS, Dang Q, Molloi S, Kassab GS. Nonuniformity of axial and circumferential remodeling of large coronary veins in response to ligation. Am J Physiol Heart Circ Physiol 2006;290:H1558-65.
9. Monos E, Kauser K, Contney SJ, Cowley AW Jr, Stekiel WJ. Biomechanical and electrical responses of normal and hypertensive veins to shortterm pressure increases. In: Bruschi G, Borghetti A, editors. Cellular aspects of hypertension. Berlin: SpringerVerlag; 1991. p. 51-7.
10. Monos E, Raffai G, Dornyei G, Nadasy GL, Feher E. Structural and functional response of extremity veins to longterm

gravitational loading and unloading—lessons from animal systems. Acta Astronaut 2007;60:406-14.
11. Rachev A, Manoach E, Berry J, Moore JE Jr. A model of stress-induced geometrical remodeling of vessel segments adjacent to stents and artery/graft anastomoses. J Theor Biol 2000;206:429-43.
12. Chen HY, Sinha AK, Choy JS, Zheng H, Sturek M, Bigelow B, et al. Mis-sizing of stent promotes intimal hyperplasia: impact of endothelial shear and intramural stress. Am J Physiol Heart Circ Physiol 2011;301:H2254-63.
13. Teebken OE, Puschmann C, Aper T, Haverich A, Mertsching H. Tissue-engineered bioprosthetic venous valve: a long-term study in sheep. Eur J Vasc Endovasc Surg 2003;25:305-12.
14. Fronek A, Criqui MH, Denenberg J, Langer RD. Common femoral vein dimensions and hemodynamics including Valsalva response as a function of sex, age, and ethnicity in a population study. J Vasc Surg 2001;33:1050-6.
15. Rittgers SE, Oberdier MT, Pottala S. Physiologically-based testing system for the mechanical characterization of prosthetic vein valves. Biomed Eng Online 2007;6:29.
16. Tien WH, Chen HY, Berwick ZC, Krieger J, Chambers S, Dabiri D, et al. Characterization of a bioprosthetic bicuspid venous valve hemodynamics: implications for mechanism of valve dynamics. Eur J Vasc Eur J Vasc Endovasc Surg 2014;48:459-64.
17. Tien WH, Chen HY, Berwick ZC, Krieger J, Chambers S, Dabiri D, et al. Hemodynamic coupling of a pair of venous valves. J Vasc Surg Venous Lymphat Disord 2013;2:303-14.
18. Brass M, Berwick ZC, Zhao X, Chen H, Krieger J, Chambers S, et al. Remodeling of canine common iliac vein in response to venous reflux and hypertension. J Vasc Surg Venous Lymphat Disord 2015;3:303-11.
19. Schneider FA, Siska IR, Avram JA. Venous wall—morphological and functional aspects. In: Clinical physiology of the venous system. New York: Springer; 2003. p. 23-76.
20. Meissner MH, Moneta G, Burnand K, Gloviczki P, Lohr JM, Lurie F, et al. The hemodynamics and diagnosis of venous disease. J Vasc Surg 2007;46:S4-24.
21. Lurie F, Kistner RL, Eklof B. The mechanism of venous valve closure in normal physiologic conditions. J Vasc Surg 2002;35:713-7.
22. Lurie F, Kistner RL, Eklof B, Kessler D. Mechanism of venous valve closure and role of the valve in circulation: a new concept. J Vasc Surg 2003;38:955-61.
23. Gusic RJ, Myung R, Petko M, Gaynor JW, Gooch KJ. Shear stress and pressure modulate saphenous vein remodeling ex vivo. J Biomech 2005;38:1760-9.
24. Hayashi K, Mori K, Miyazaki H. Biomechanical response of femoral vein to chronic elevation of blood pressure in rabbits. Am J Physiol Heart Circ Physiol 2003;284:H511-8.
25. Zilla P, Moodley L, Scherman J, Krynauw H, Kortsmit J, Human P, et al. Remodeling leads to distinctly more intimal hyperplasia in coronary than in infrainguinal vein grafts. J Vasc Surg 2012;55:1734-41.
26. Kraiss LW, Geary RL, Mattsson EJ, Vergel S, Au YP, Clowes AW. Acute reductions in blood flow and shear stress induce platelet-derived growth factor-A expression in baboon prosthetic grafts. Circ Res 1996;79:45-53.
27. Fung YC, Fronek K, Patitucci P. Pseudoelasticity of arteries and the choice of its mathematical expression. Am Physiol Soc 1979;237:H620-31.

Submitted May 22, 2016; accepted Aug 5, 2016.

Additional material for this article may be found online at www.jvsvenous.org.

APPENDIX (online only).

A vein is modeled as a thin-walled tube by a two-dimensional strain energy function[25]:

$$W = \frac{C}{2}\left(\exp\left[a_1 E_\theta^2 + a_2 E_z^2 + 2a_4 E_\theta E_z\right] - 1\right) \tag{A1}$$

where $C\,[kPa]$, a_1, a_2, a_4 are material constants; E_θ and E_z are, respectively, the normal components of the Green-Lagrange strain tensor **E** in the circumferential and axial directions of the vessel. The Lagrange stress tensor **S** is defined as

$$\mathbf{S} = \frac{\partial W}{\partial \mathbf{E}} \tag{A2}$$

If we carry out the derivation, we obtain the components of the Lagrange stress tensor as

$$S_\theta = C(a_1 E_\theta + a_4 E_z)\exp\left[a_1 E_\theta^2 + a_2 E_z^2 + 2a_4 E_\theta E_z\right] \tag{A3.1}$$

$$S_z = C(a_4 E_\theta + a_2 E_z)\exp\left[a_1 E_\theta^2 + a_2 E_z^2 + 2a_4 E_\theta E_z\right] \tag{A3.2}$$

It follows that the Cauchy stress tensor components are

$$\begin{aligned}\sigma_\theta &= \lambda_\theta^2 S_\theta \\ &= C(2E_\theta + 1)(a_1 E_\theta + a_4 E_z)\exp\left[a_1 E_\theta^2 + a_2 E_z^2 + 2a_4 E_\theta E_z\right]\end{aligned} \tag{A4.1}$$

$$\begin{aligned}\sigma_z &= \lambda_z^2 S_z \\ &= C(2E_z + 1)(a_4 E_\theta + a_2 E_z)\exp\left[a_1 E_\theta^2 + a_2 E_z^2 + 2a_4 E_\theta E_z\right]\end{aligned} \tag{A4.2}$$

where $\lambda_i = \sqrt{2E_i + 1}, \quad (i = \theta, z)$ are stretch ratios. By using Laplace's law for thin-walled tube, ie,

$$\sigma_\theta = \frac{Pr}{t} \tag{A5}$$

where *P* is the transmural blood pressure and *r* and *t* are the current inner radius and wall thickness of the deformed vessel, we obtain the modeled pressure as

$$\begin{aligned}P &= \frac{t\sigma_\theta}{r} \\ &= \frac{tC(2E_\theta + 1)(a_1 E_\theta + a_4 E_z)\exp\left[a_1 E_\theta^2 + a_2 E_z^2 + 2a_4 E_\theta E_z\right]}{r}\end{aligned} \tag{A6}$$

The resultant axial force in the vessel wall, again based on the thin-wall assumption, is given by

$$F = 2\pi t\left(r + \frac{t}{2}\right)\sigma_z - \hat{P}\pi r^2 \tag{A7}$$

where $\hat{P}$ is the measured intraluminal pressure.

The best-fit values of the material constants C, a_1, a_2 and a_4 were estimated in the least-square sense by minimizing the cost function

$$\Phi = \sum_{i=1}^{N}\left(P - \hat{P}\right)^2 + \left(F - \hat{F}\right)^2 \tag{A8}$$

where $\hat{F}$ is the measured axial force and N is the total number of data points.